

Characterizing the Diurnal Signature in Two Way Satellite Time Transfer (TWSTT) Data with a Kalman Filter

Demetrios Matsakis, *U.S. Naval Observatory*

BIOGRAPHY

Dr Demetrios Matsakis is Chief Scientist for Time Services at the US Naval Observatory (USNO). He received his undergraduate degree in Physics from MIT. His PhD was from U.C. Berkeley, and his thesis, under Charles Townes, involved building masers and using them for molecular radio astronomy and interferometry. Hired at the USNO in 1979, he measured Earth rotation and orientation using Connected Element Interferometry and Very Long Baseline Interferometry (VLBI). Beginning in the early 90's, he started working on atomic clocks and in 1997 was appointed Head of the USNO's Time Service Department. He has over 100 publications, has served on many international commissions, and for three years was President of the International Astronomical Union's Commission on Time. Email: demetrios.matsakis@usno.navy.mil;

ABSTRACT

This purpose of this paper is to call further attention to the technique of using a Kalman filter [1] to estimate the diurnal signature in TWSTT data. Accordingly, we have reduced all publicly available data since 2004 on inter-Europe and Europe-North American baselines [2], for site pairs as well as triplets. Variations in the diurnal amplitude and phase are easily identified, including some that are too weak to be identified by simple inspection. Changes in the variations of the amplitude and phase of the diurnals in the TAI-generating observations are evident when the chip rate and bandwidth were reduced in 2009 (MJD 55042) and the bandwidth was further reduced in 2011 (MJD 55769), as indicated in Table 1. This technique would be a useful tool when used in conjunction with less readily-available information, both meteorological and instrumental.

INTRODUCTION

TWSTT (also referred to with the acronym TWSTFT), is extensively used by the International Bureau of Weights and Measures (BIPM) in the generation of Coordinated

Universal Time (UTC), either directly or as the source of calibration accuracy in combination with GNSS data. However, the existence of diurnals, often at the level of 1 ns, could also be an indicator of the accuracy of the calibration, particularly as diurnal temperature variations are often less than seasonal temperature variations.

Many theories have been proposed to explain the diurnals, and some have had limited success. For example, unmodelled satellite orbits have been shown to be the cause of some diurnals in Asian links [3], unmodelled ionosphere at times of high Total Electron Content (10^{18} electrons/m² at the daytime station) was computed to result in diurnals in trans-Atlantic observations whose amplitudes ranged from ~ 40 ps to ~1 ns (worst-case) [4], and seasonal variations of diurnal strength have also been at times reported [5]. Diurnals have been associated with equipment and bandwidth changes, and some are reported herein.

Very recently diurnals been reported in closure sums involving all baselines associated with certain site triplets, but not others [6]. (The closure sum of data between sites A, B, and C is the sum of their individual baseline clock difference observations, which can be written A-B, B-C, and C-A.) While no source of single-baseline diurnals would be 100% cancelled in the closure sums since the pairwise observations are not made at precisely the same time, the existence of diurnals in closure sums might plausibly limit the diurnal contribution from effects to which closure sums are insensitive (such as clock, orbit, and ionosphere variations, as well as many forms of instrumental calibration variations, particularly if only one satellite transponder is involved). However, if the existence of variable closure sums indicates that each baseline is unequally and differently weighting portions of its bandwidth; hence temperature, ionosphere, and instrumental variations need not necessarily be ruled out. Signal confusion is an example of an effect that closure sums would not eliminate, yet this particular effect would not normally be expected to mimic a diurnal signature since the observing schedule is the same for every hour

observations are made. It could however do so in combination with temperature-related effects.

A motivation for the use of Kalman filters is that, although of the listed plausible causes only satellite orbital variations can be exactly modelled with a single sinusoid, Kalman filters have been useful in eliminating short-term variations in TWSTT, as have other techniques such as use of Vondrak smoothing in combination with GNSS data [7-8]. Sweden's timing lab SP routinely reduces data with a diurnal-removing Kalman filter, and as a great service to the community makes all its results available on <http://igsrt.sp.se/twstft>. USNO also uses this technique in its internal reductions of the USNO-AMC TWSTT link [9].

Perhaps because of the great difficulty in quantifying diurnal effects, as well as in gathering quantitative ancillary information, a definitive cause for diurnal signatures has yet to be universally agreed upon. The purpose of this paper is to explore the power of Kalman filters in quantifying diurnals.

DATA ANALYSIS

This work is based upon 12 years of data gathered from individual laboratory public or password-protected data servers, the BIPM's data server, and four years of internal USNO data linking USNO-DC with the Alternate Master Clock (AMC) in Colorado Springs, Colorado. Reductions of ITU-R formatted files were made following standard techniques, with minimal outlier removal. Closure sums were generated from summing all possible site triplets (LabA-LabB) + (LabB-LabC) + (LabC-LabA). Only operational data that were taken within an hour of each other were used in the summation.

A Kalman filter was applied to the data, employing both forward and backwards solutions. The Kalman filter fit to the diurnal sine and cosine variations, as well as the overall time and frequency difference; the amplitude of a diurnal is the square root of the sum (RSS) of the sine and cosine parameters, and the diurnal's phase is the arctangent of their ratio. In each direction, initial conditions were determined using a least-squares fit to the ten end-points, which were then discarded. Each individual datum's uncertainty was the standard deviation of the 1-second points going into the longer-duration value used (two minutes' worth for UTC data); the root-sum-square (rss) of this was used for closure triplets. The process noises (Q) were such that the fitted parameters would be 50% adjusted about two days after an abrupt variation in them. Numerically, the Q 's were 10^{-4} ns 2 for clock differences, 10^{-2} (ns/day) 2 for frequency, and 210^{-2} for the sinusoidal terms; slightly lower ones were employed for the USNO-AMC observations. These parameters were not optimized, but the solutions appeared

fairly insensitive to reasonable changes in their values. Confidence was provided by the consistency of the fitted diurnal phases, as well as by inspection of the superimposition of the fitted sinusoidal term upon the data themselves.

Corrections for the ionosphere delay were not applied to the data, since they are not applied by the BIPM. However the effect on the trans-Atlantic baselines was estimated using ionosphere estimates from the Center for Orbit Determination in Europe (CODE). We found that in Europe-only baselines the effects were a few tens of picoseconds, while over trans-Atlantic baselines the RMS error approached 100 ps over the last few years. This is significant; although we show below that it is not enough to explain the observed diurnals.

RESULTS/DISCUSSION

Figure 1 shows raw and fitted data from two nearly collocated antennas at the USNO; this could be considered a validation of the ability of the filter, as parameterized, to reliably identify a diurnal of 200 ps peak to peak within the noisy data.

Figure 2 illustrates the decreasing diurnal signature in TWSTT data between the USNO and the German timing lab PTB since August 2011. The red curve shows that the phase of the diurnal has stayed near -100 degrees. The expected delay due to the uncorrected ionosphere is shown in the green curve; its phase from -10 to -40 degrees. The ionosphere's effect was computed using the well-known formula for zenith delay (Zdelay):

$$Zdelay \text{ (meters)} = 40.3 * 10^{16} * TECU / f_{\text{Hz}}^2 \quad (1)$$

, where TECU is the Total Electron Content (TEC) in units of 10^{16} electrons/m 2 [10]. Converting to nanoseconds and expressing the frequency in GHz, one obtains

$$Zdelay \text{ (ns)} = 1.34 * TECU / f_{\text{GHz}}^2 \quad (2)$$

Figures 3 show that the progressively weaker diurnals become harder to see by eye in the raw data, and Figure 4 superimposes data from the early period of large diurnals onto more recent data with smaller diurnals.

Figures 5 and 6 show the amplitude and phase between the Swiss timing lab METAS and Germany's timing lab PTB. The phase variation of Figure 6 is strong enough to be easily confirmed by inspection (Figures 7 and 8).

Variable diurnal signatures on two trans-Atlantic triplets including the US and German timing labs NIST and PTB are shown in Figures 9 and 10; sections of the timing data are expanded in Figures 11 and 12. Clearly the diurnals are not constant even in closure sums. The phase plot of

Figure 10 does not include earlier times because the phase variations are much more variable, while the amplitude of the diurnals was somewhat less but also more variable.

Figures 13-16 are admittedly “busy”. They are an overlay of all closure sums associated with the PTB and either OP (France), SP (Sweden), NIST, or USNO respectively. They are presented to indicate what kind of big-picture conclusions might be inferable. The increase in diurnals after MJD 55042, when the bandwidth and chip rate were reduced, is evident, but not a further reduction of bandwidth on MJD 55769. Figures 17 and 18 show that changes in the diurnals' phase patterns also occurred, perhaps the trans-Atlantic ones changed at both times.

For completeness, the last figure shows an ionosphere calculation at time of large TEC.

CONCLUSIONS FOR FURTHER WORK

Speculation on the causes of diurnal effects can be substantiated by associating the fitted diurnal parameters with times of satellite, frequency, bandwidth, or chip rate, changes, known or inferred satellite orbit variations, equipment changes, schedule changes, ionosphere total electron content (TEC), time of year, carrier to noise (CNO) ratios, signal-to-noise (SNR) ratios, and site and/or equipment temperatures, humidities, and pressures. All this information is not available now, but could become so. Such efforts are labor intensive, but not beyond the scope of researchers and students.

NOTE IN PROOF

At a side-meeting of the BIPM/CCTF Working Group on TWSTT, Dr. Calvin Lin announced that TWSTT data reduced digitally using software developed by Taiwan's (TL) do not display the diurnal signature present in parallel observations with the analog modem design used for the data presented herein. Furthermore, Dr. Thorsten Feldmann stated that these diurnals were explained as part of the ACES project (Atomic Clock Ensemble in Space) as due to receiver tracking loops effectively locking to different Doppler-shifted frequencies over the satellite's daily orbital cycle, but that the net effect would cancel in digital reductions because the loop characteristics would be software defined and completely identical at both stations. Nothing in this paper is inconsistent with these revelations. The net effect of eliminating diurnals will be to allow TWSTT data to better complement GPS data on daily and subdaily scales, although significant improvements and understanding of GPS time transfer are hereby acknowledged [11-13].

ACKNOWLEDGMENTS

We thank the international TWSTT community, the BIPM, and the USNO TWSTT team for making their data available.

For creating Table 1, we are pleased to thank Victor Zhang of NIST, who is currently president of the BIPM's TWSTFT Working Group.

REFERENCES

- [1] N. Kalouptsides, “Signal Processing Systems”, John Wiley and Sons, 1997.
- [2] For example, directories below TimeLink/LkC/LongTerm inb ftp://tai.bipm.org
- [3] W.H. Tseng, K.M. Feng, S.Y. Lin, H.T. Lin, Y.J. Huang, and C.S. Liao, “Sagnac effect and diurnal correction on two-way satellite time transfer,” 2011, IEEE Trans. Instr. Meas., vol. 60, no. 7, pp 2298-2303
- [4] D. Kirchner, 1999, “Two Way Satellite Time and Frequency Transfer”, Reviews of Radio Science, pp. 27-44
- [5] D. Matsakis, K. Senior, and P. Cook, 2002, “Comparison of Continuously Filtered GPS Carrier Phase Time Transfer with Independent GPS Carrier-Continuously Filtered GPS Carrier Phase Time Transfer with Independent GPS Carrier-Washington, D.C., pp 63-87
- [6] V. Zhang, 2015, NIST Station Report to 23rd Meeting of the CCTF Working Group on TWSTFT
- [7] Vondrak and Cepek, 2000, “Combined smoothing and its use in combining Earth orientation parameters measured by space techniques”, Astron. Astroph. Sup., Ser 147, pp 347-359
- [8] D. Matsakis, G. Petit, and G. Panfilo, “Vondrak Smoothing”, Sixth International Timescale Algorithm Symposium, 2015, Paris, France, September 9-11 2015.
- [9] P. Koppang and J. Skinner, private communication
- [10] http://www.navipedia.net/index.php/Ionospheric_Delay.
- [11] J. Yao, I. Skakun, Z. Jiang, and J. Levine, “A detailed comparison of two continuous GPS carrier-phase time transfer techniques”, Metrologia 52, 2015, pp. 666-676.
- [12] J. Yao, J. Levine, and M. Weiss “Towards continuous GPS carrier-phase time transfer: eliminating the time discontinuity at an anomaly”, J. Res. of NIST, 120, pp. 280-292, 2015.
- [13] J. Yao, M. Weiss, C. Curry, and J. Levine, “GPS Jamming and GPS Carrier-Phase Time Transfer”, these proceedings (ION-PTTI, 2016)

History of Transatlantic TWSTFT Parameters (NIST records from 2001)

| SAT ID | LINK ID | Operation Period | BW (MHz) | Chip-rate (Mchip/s) | US Stations' Frequency (MHz) | | Europe Stations' Frequency (MHz) | | MODEM |
|--------|---------|---|----------|---------------------|------------------------------|------------|----------------------------------|------------|--------------|
| | | | | | Up Link | Down Link | Up Link | Down Link | |
| IS-706 | 4 | 2001-01-01 (51910) - 2001-04-03 (52002) | 3.7 | 2.5 | 14220.5475 | 11925.5475 | 14220.5475 | 12729.8000 | MITREX |
| IS-706 | 4 | 2001-04-04 (52003) - 2003-09-15 (52897) | 3.7 | 2.5 | 14392.0030 | 11592.0000 | 14392.0000 | 11592.0000 | MITREX/SATRE |
| IS-903 | 6 | 2003-09-16 (52898) - 2005-05-08 (53498) | 3.7 | 2.5 | 14349.5770 | 11542.2200 | 14342.2200 | 11549.5770 | SATRE |
| IS-707 | 6 | 2005-05-09 (53499) - 2006-10-24 (54032) | 3.7 | 2.5 | 14461.2000 | 11461.2000 | 14261.2000 | 11461.2000 | SATRE |
| IS-707 | 9 | 2006-10-25 (54033) - 2008-02-05 (54501) | 3.7 | 2.5 | 14211.7500 | 11916.7500 | 14211.7500 | 12716.7500 | SATRE |
| IS-3R | 11 | 2008-02-06 (54502) - 2009-07-29 (55041) | 3.7 | 2.5 | 14375.0500 | 12030.7500 | 14330.7500 | 12627.0500 | SATRE |
| T11-N | 13 | 2009-07-30 (55042) - 2011-07-26 (55768) | 2.5 | 1 | 14285.5500 | 11726.5500 | 14026.5500 | 11485.5500 | SATRE |
| T11-N | 15 | 2011-07-27 (55769) - 2011-08-02 (55775) | 1.6 | 1 | 14298.4300 | 11746.5900 | 14046.5900 | 11498.4300 | SATRE |
| T11-N | 16 | 2011-08-03 (55776) - 2016-07-26 (57595) | 1.6 | 1 | 14289.0600 | 11746.5900 | 14046.5900 | 11489.0600 | SATRE |

| | | |
|---|---|--|
| (1) 2001-01-01 (51910) - 2003-05-11 (52770) | 14:00 UTC on Monday, Wednesday and Friday | PS: IEN, NIST, NPL, PTB, VSL, USNO |
| (2) 2003-05-12 (52771) - 2004-04-27 (53122) | 14:00 UTC daily | PS: IEN, NIST, NPL, OCA (52848), OP (52848), PTB, ROA, SP (53012), VSL, USNO |
| (3) 2004-04-28 (53123) -2005-05-04 (53494) | 0:00-16:00 UTC daily | PS: CH (53381), IEN, IPQ (53684), NIST, NPL, OCA (52848), OP (52848), PTB, ROA, SP (53012), VSL, USNO |
| (4) 2005-05-05 (53495) - current | 0:00 - 22:00 UTC daily | PS: AOS (54081), CH (53381), IEN, IPQ (53684), NIST, NPL, OCA (52848), OP (52848), PTF1 (), PTF2 (), PTB, ROA, SP (53012), TIM (55977), USNO |

Table 1. Configurational changes in international TWSTT for UTC Generation, courtesy V. Zhang (NIST).

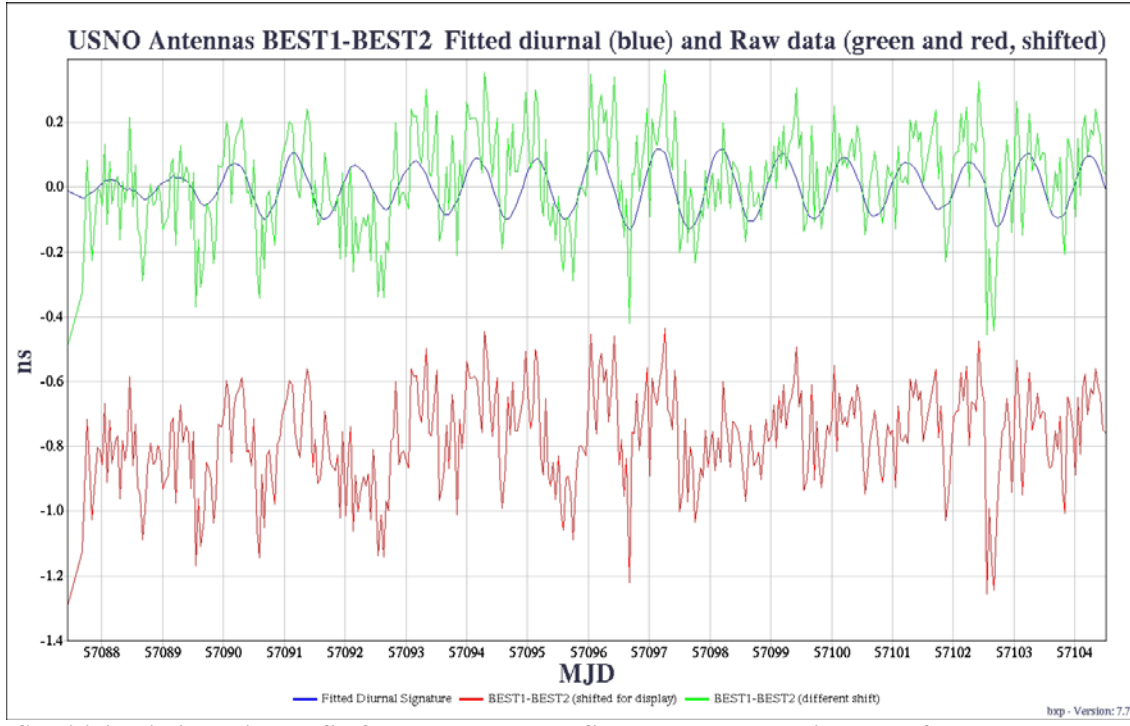


Figure 1. Sensitivity limit to diurnal fit, for chosen Kalman filter parameters. Time transfer data between two nearly collocated systems at the USNO are shifted for display and shown twice; superimposed upon the upper curve is the fitted diurnal (blue).

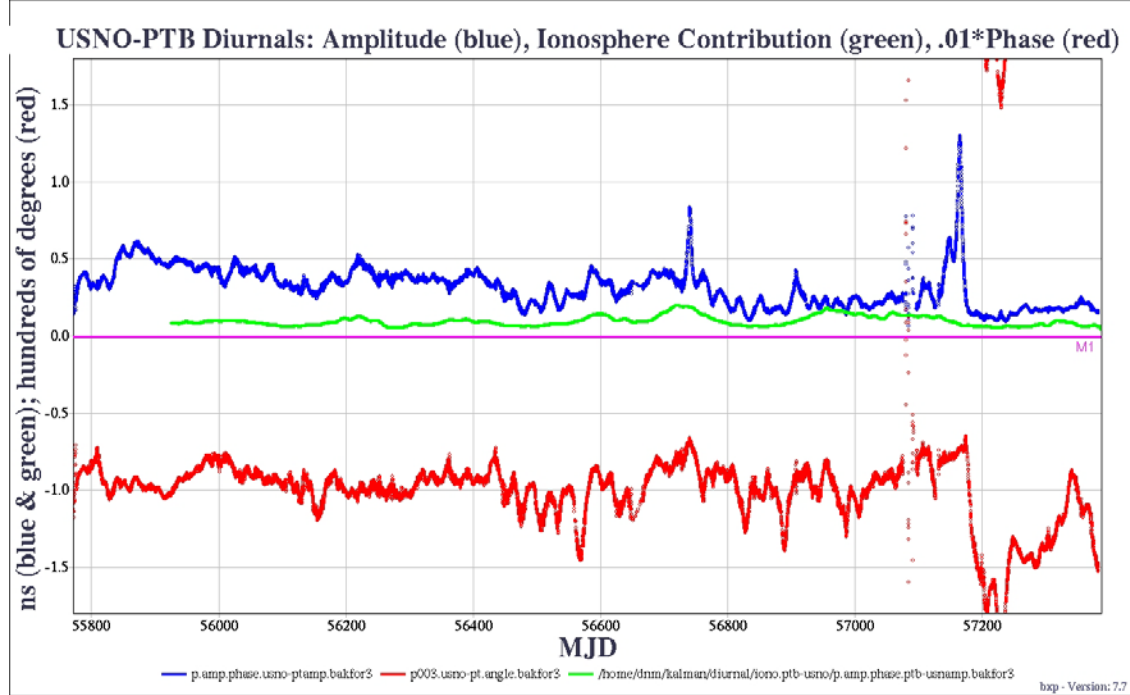


Figure 2. The generally decreasing amplitude of USNO-PTB diurnals is shown in the upper part. The USNO installed a new system on MJD 55763, and a further upgrade was implemented on MJD 57204. These dates do not correspond to any of the abrupt changes in the plot. The high-lying red points after MJD 57200 reflect the 360-degree ambiguity in phase data. The expected diurnal signature due to the ionosphere is shown in green; its phase varies from -50 to -10 degrees, consistent with the lower satellite elevation at the PTB.

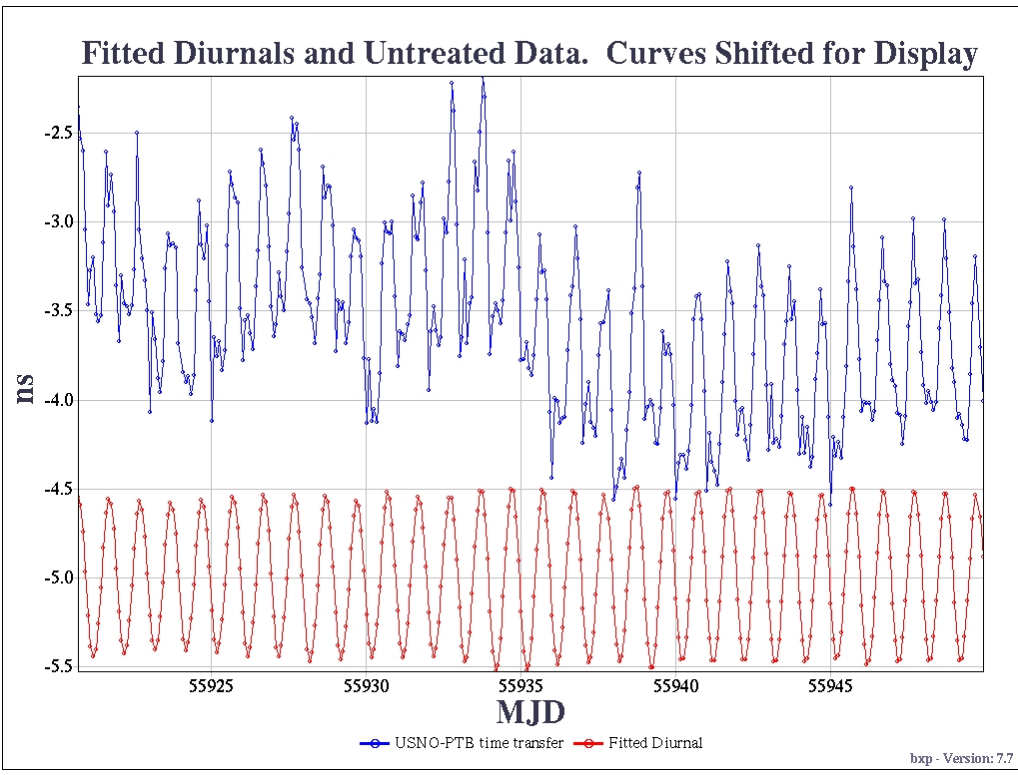


Figure 3a. USNO-PTB time transfer data and fitted diurnals about MJD 55935.

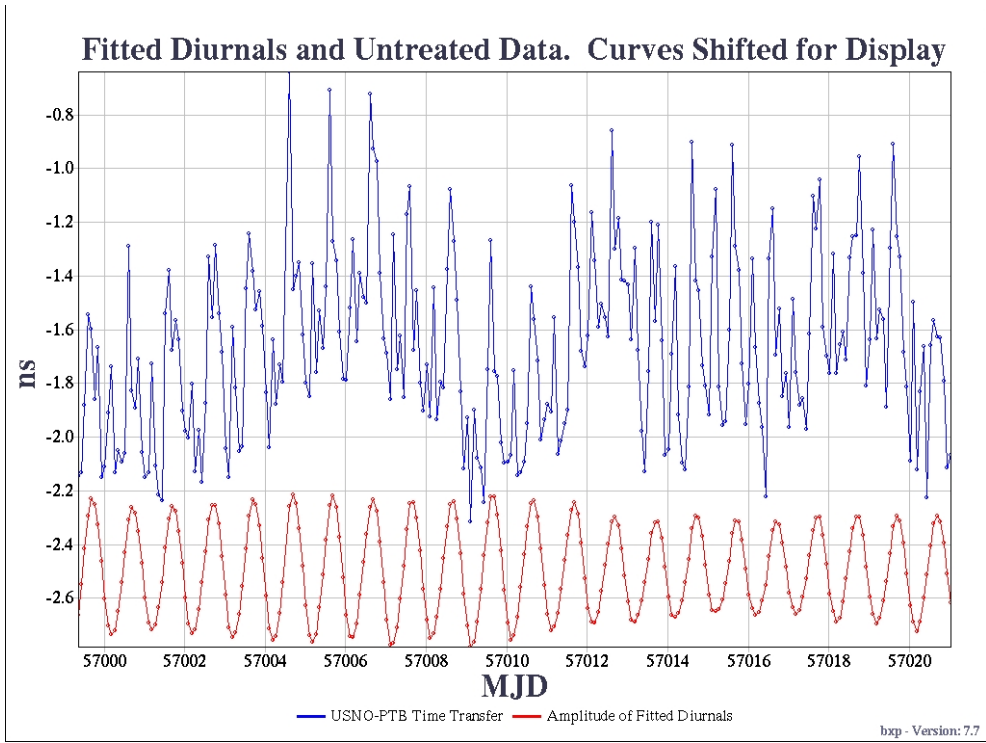


Figure 3b. USNO-PTB time transfer data and fitted diurnals about MJD 57010. Note the decreased amplitude of the diurnals.

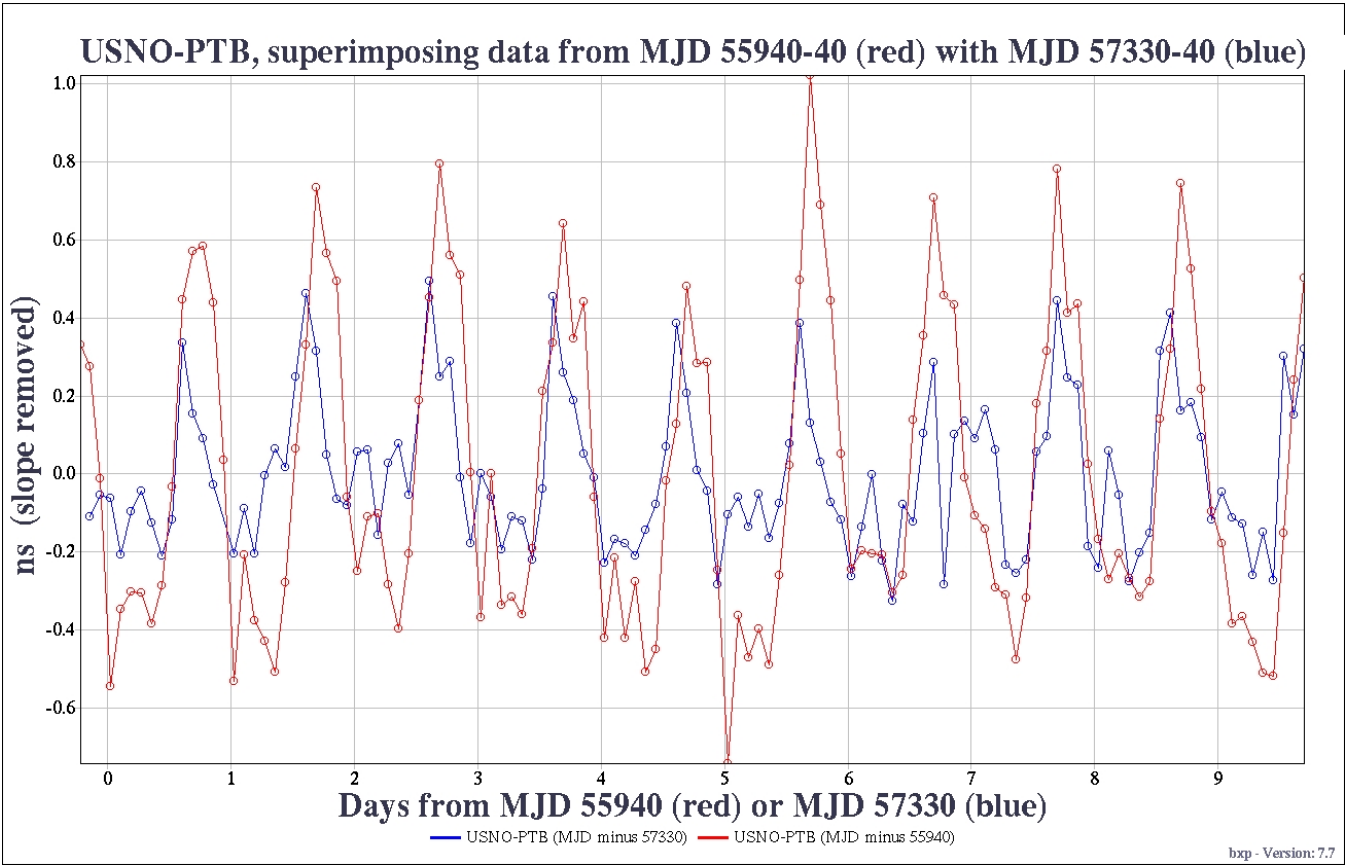


Figure 4 Data from January, 2012 superimposed upon data from October 2015, for the purpose of illustrating the change in amplitude and phase of the diurnals on the USNO-PTB baseline.

bxp - Version: 7.7

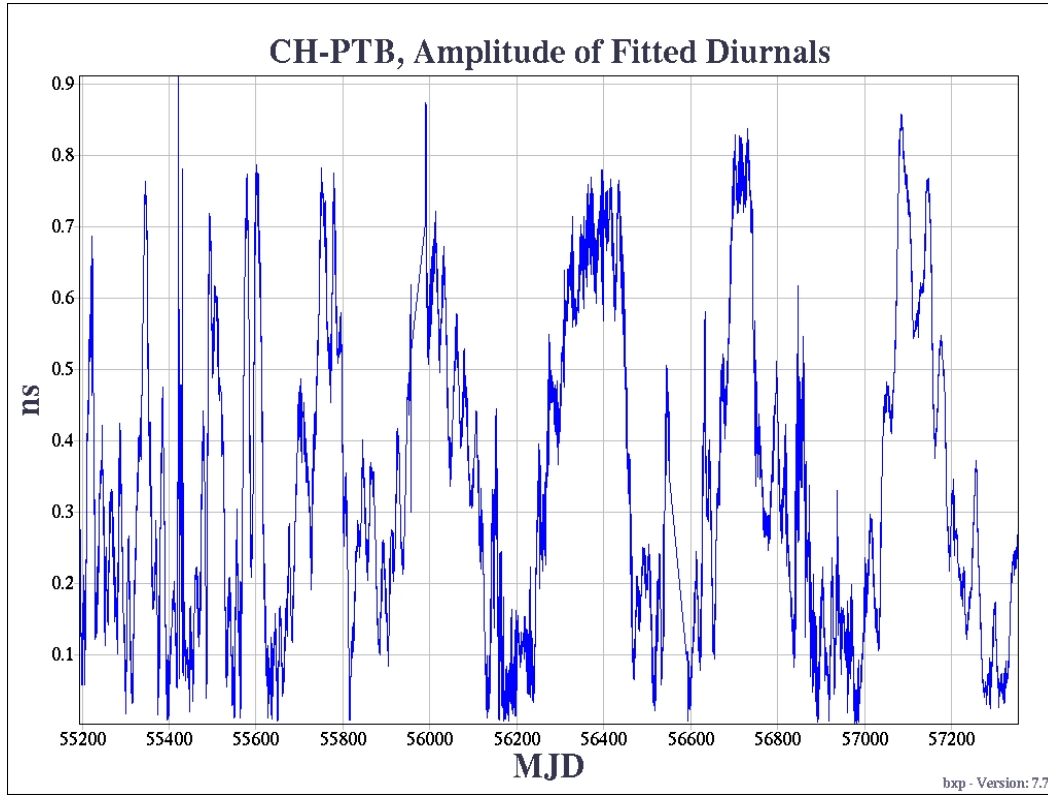


Figure 5. Amplitude of diurnals on the link between the timing labs METAS (CH) and the PTB. METAS is located in Berne, Switzerland and the PTB at Braunschweig, Germany.

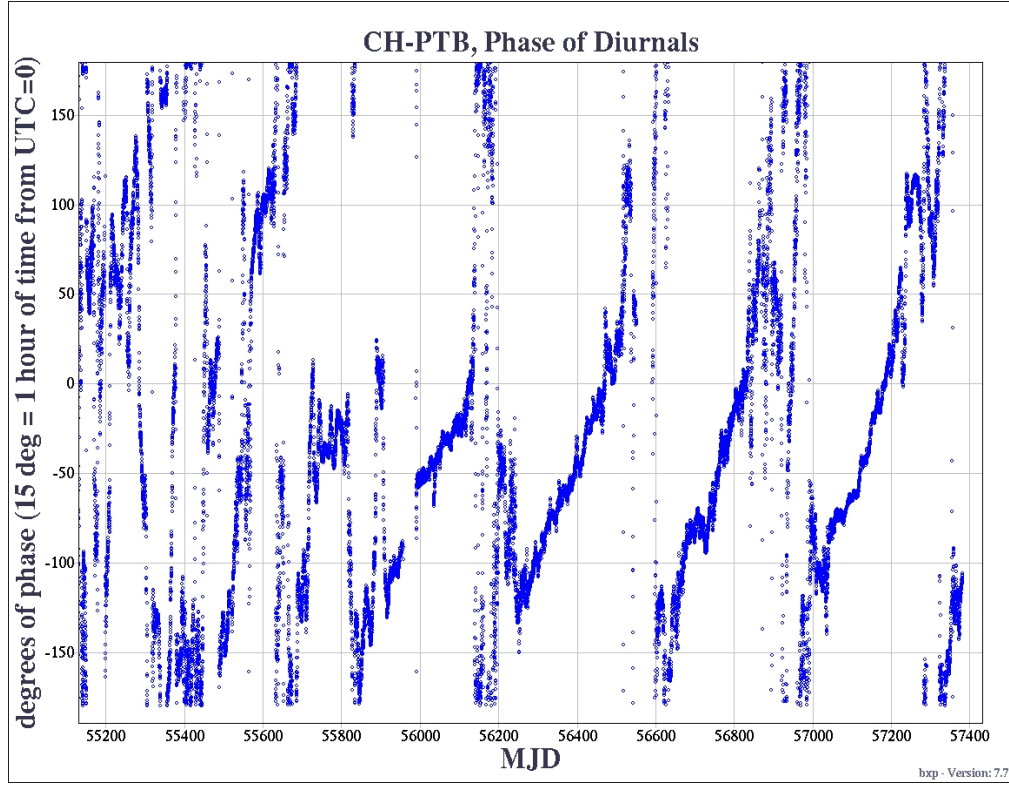


Figure 6. Phase of the diurnals on the CH-PTB baseline. The 24-hour period of the diurnals extends over 360 degrees of phase. The observation bandwidth reduced to 1.6 MHz on MJD 55769.

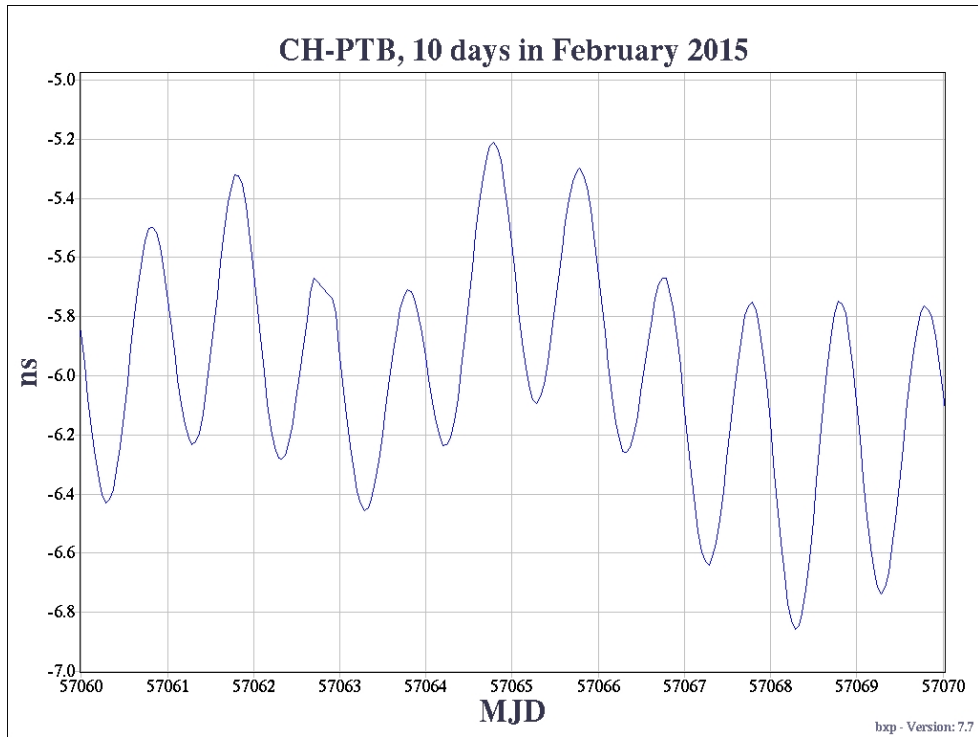


Figure 7. TWSTT time transfer data as processed by the BIPM and output on their anonymous ftp server. The peaks are seen to come at about the beginning of the last quarter of each day (as measured by MJD).

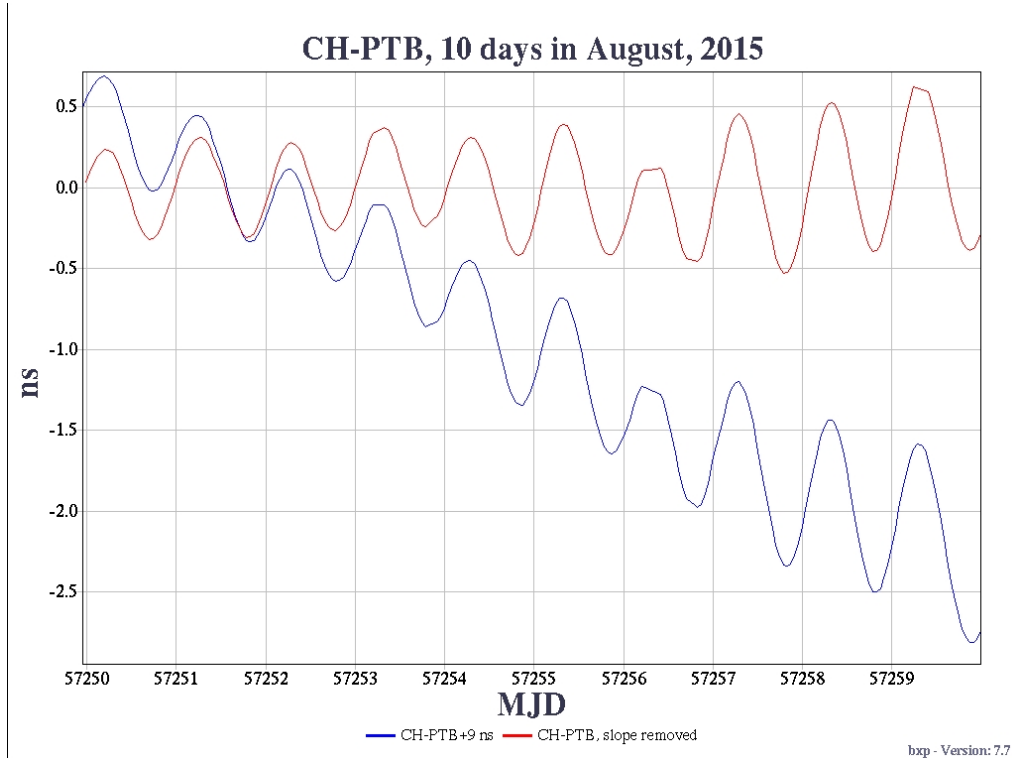


Figure 8. Time Transfer data from August, 2015. The blue curve is the raw data shifted for display, and the second curve is the raw data after removal of a linear term. In contrast to the previous figure, the highest points of the diurnals are now at the end of the first quarter of each MJD day.

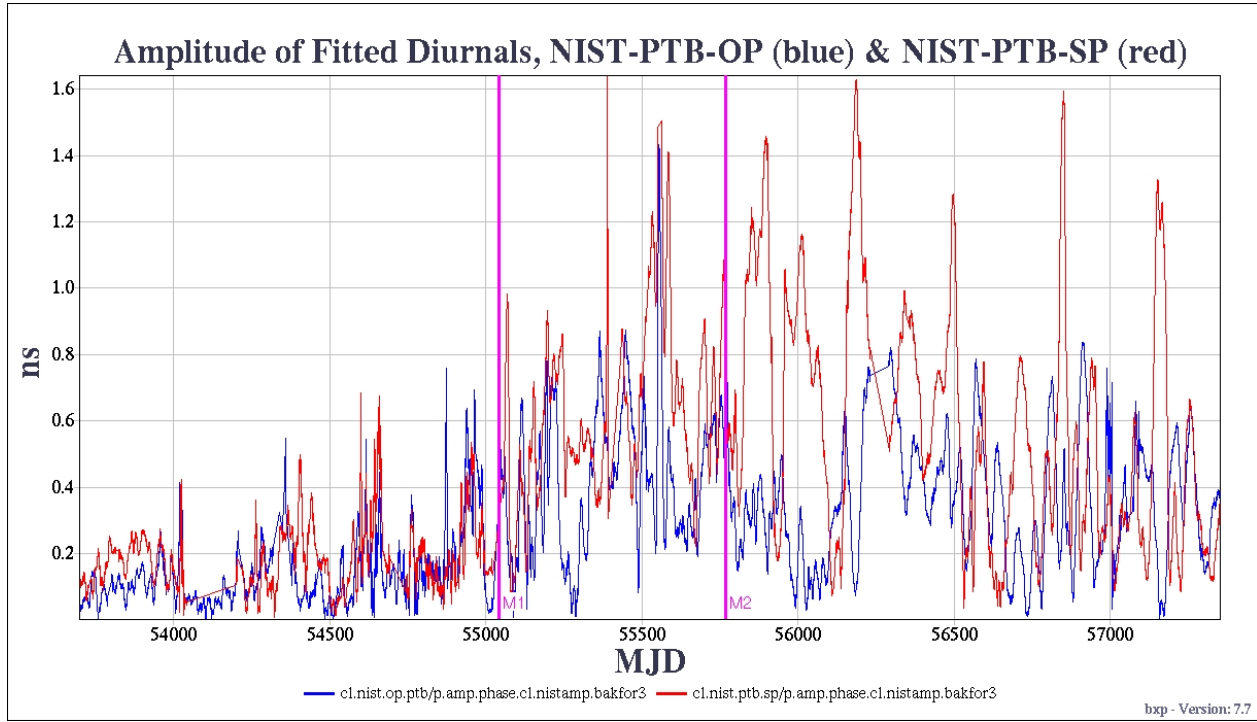


Figure 9. Variations of diurnal amplitudes for two triplets involving NIST and PTB. Blue vertical markers identify MJD 55042 and 55769, when bandwidths and/or chip rates were reduced.

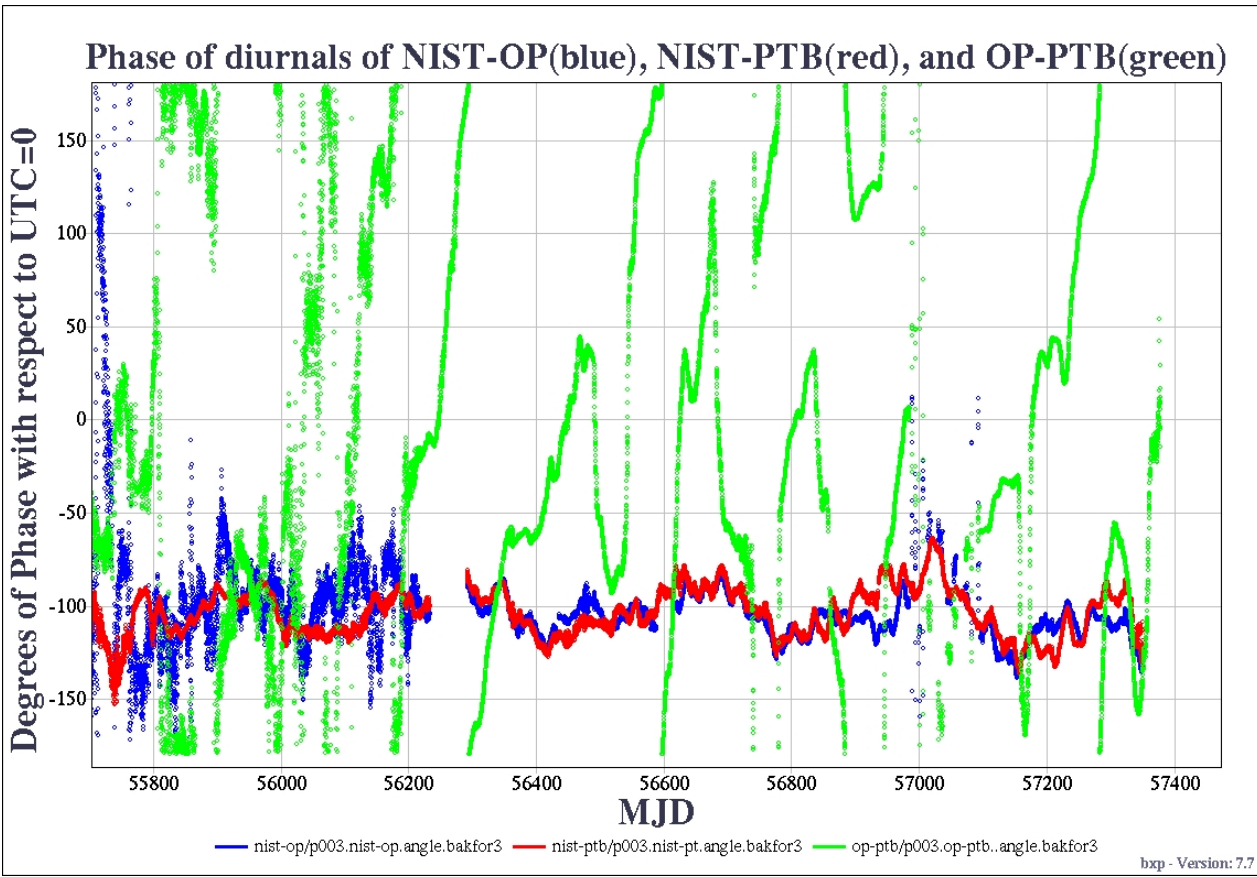


Figure 10. Phase of the diurnals on the NIST-OP-PTB baselines. The OP-PTB variations are typical for inter-European baselines. Earlier data show larger phase variations, partially because the diurnal amplitudes were less.

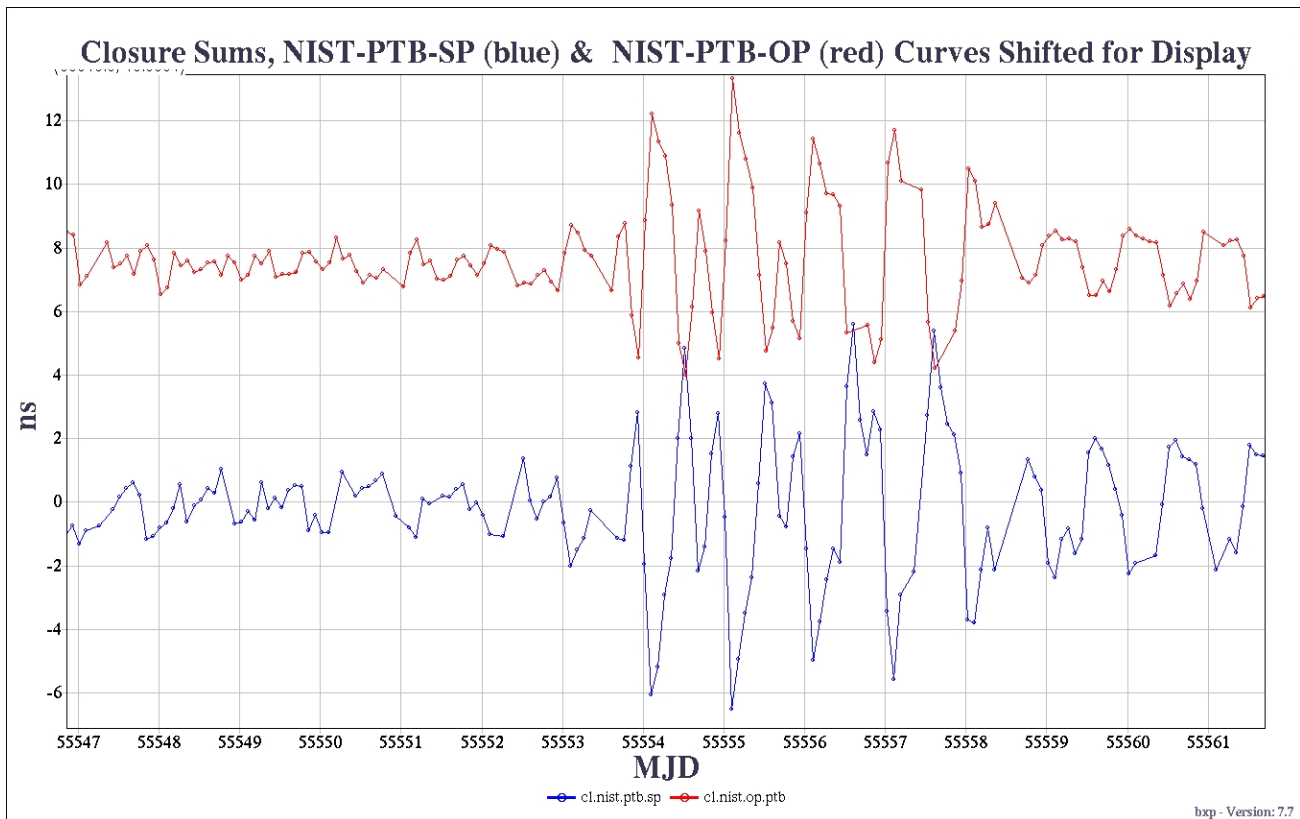


Figure 11. The two closure sums in December 2010.

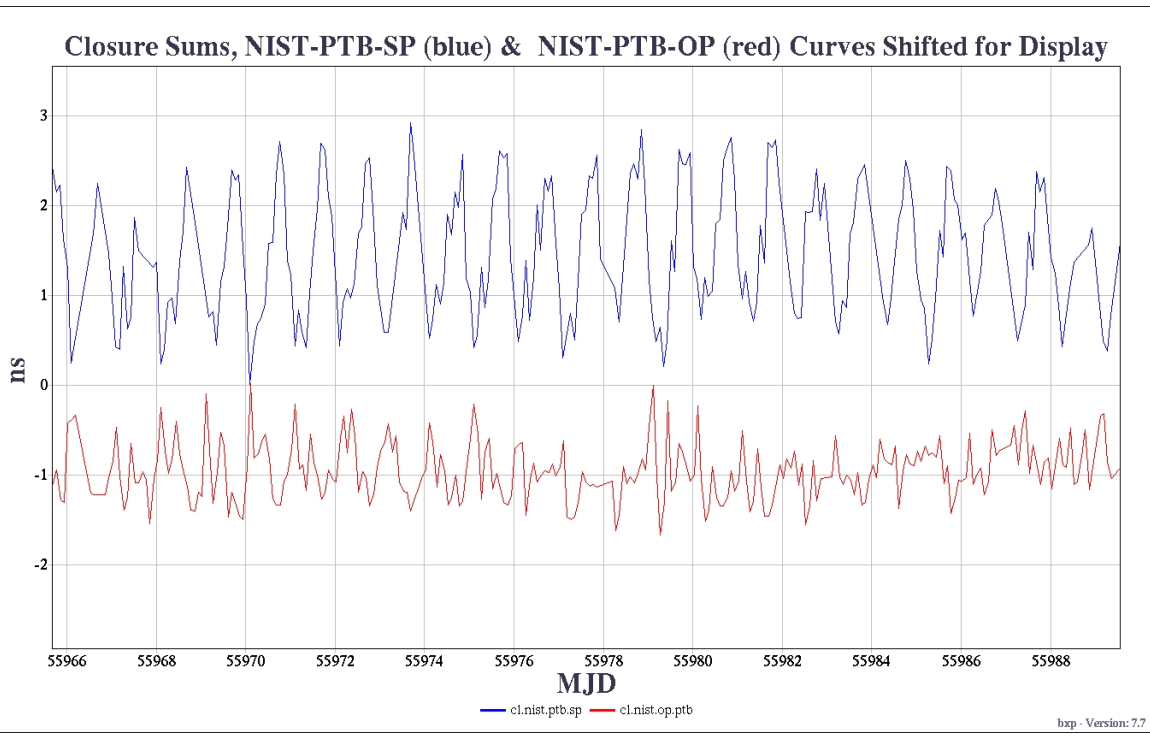


Figure 12. The two closure sums in February, 2012

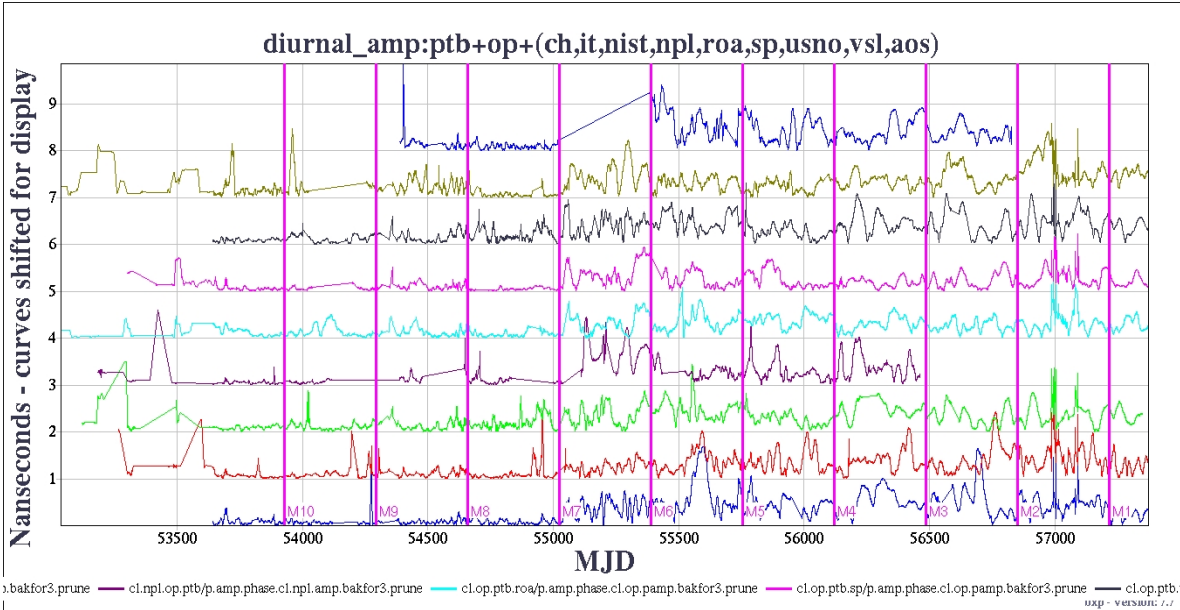


Figure 13. Closure sums for lab triplets including PTB and OP. The markers indicate July 14 of successive years. In this and successive figures, a significant increase occurred on MJD 55042 (July 30, 2009) when a satellite change resulted in reduced chip rate (1 MHz) and reduced bandwidth (2.5 MHz). A further reduction in bandwidth to 1.6 MHz on MJD 55769 (July 27, 2011) did not have an obvious effect on diurnal amplitude.

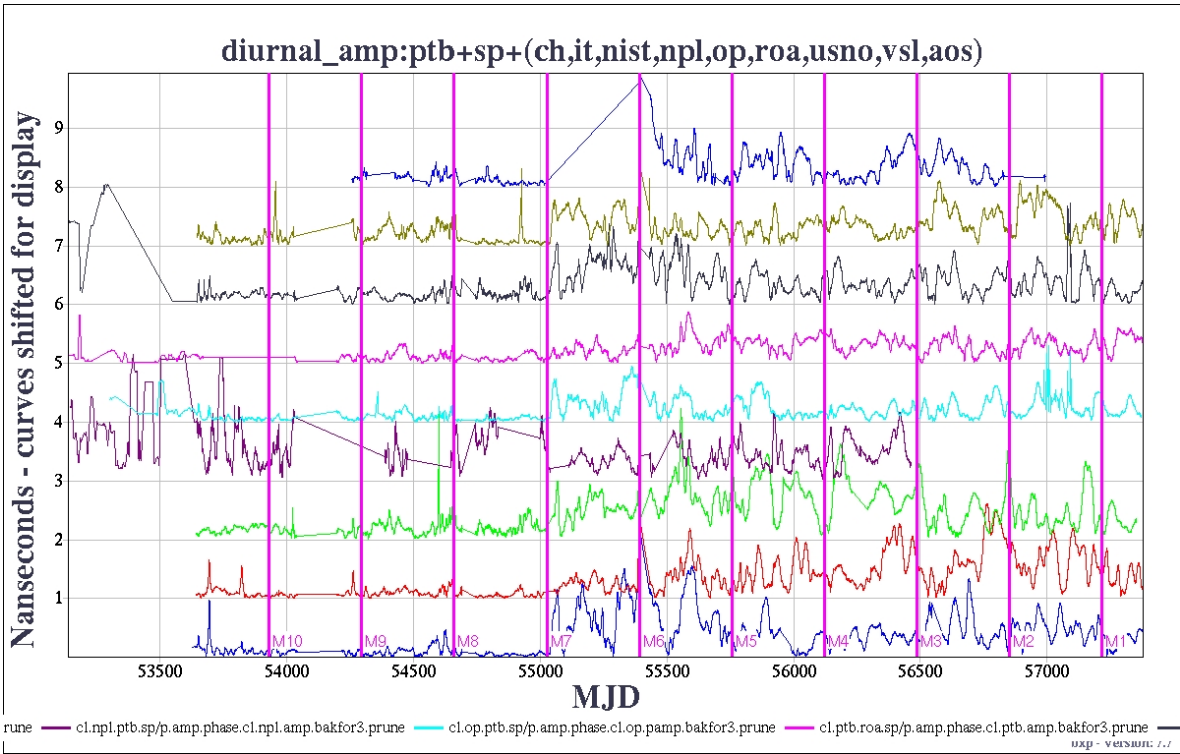


Figure 14. Closure sums for lab triplets including PTB and SP; every July 14 is marked.

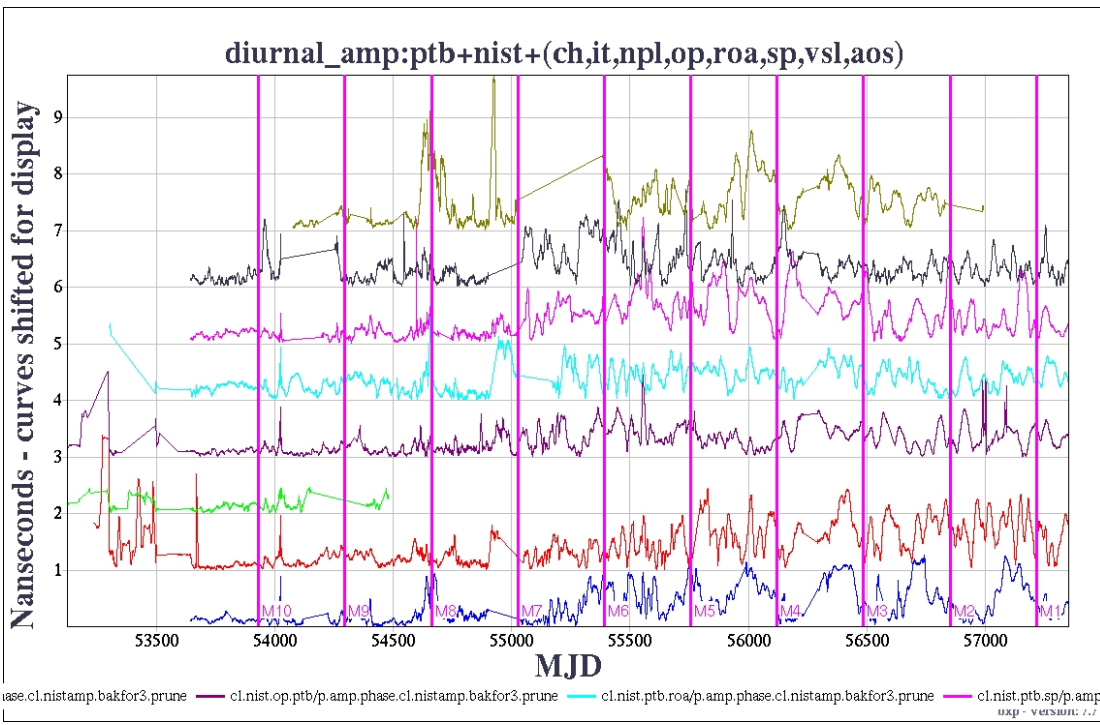


Figure 15. Closure sums for lab triplets including PTB and NIST; every July 14 is marked.

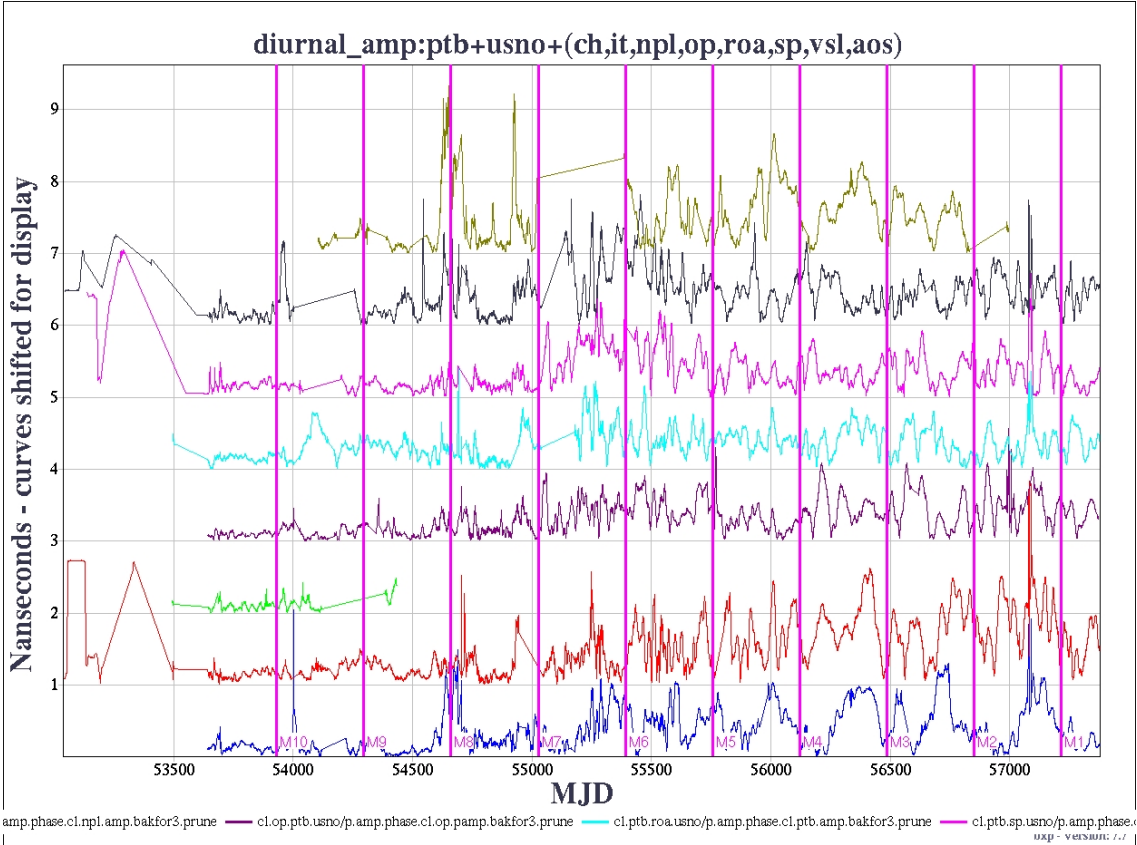


Figure 16. Closure sums for lab triplets including USNO, PTB, and one other European lab; every July 14 is marked.

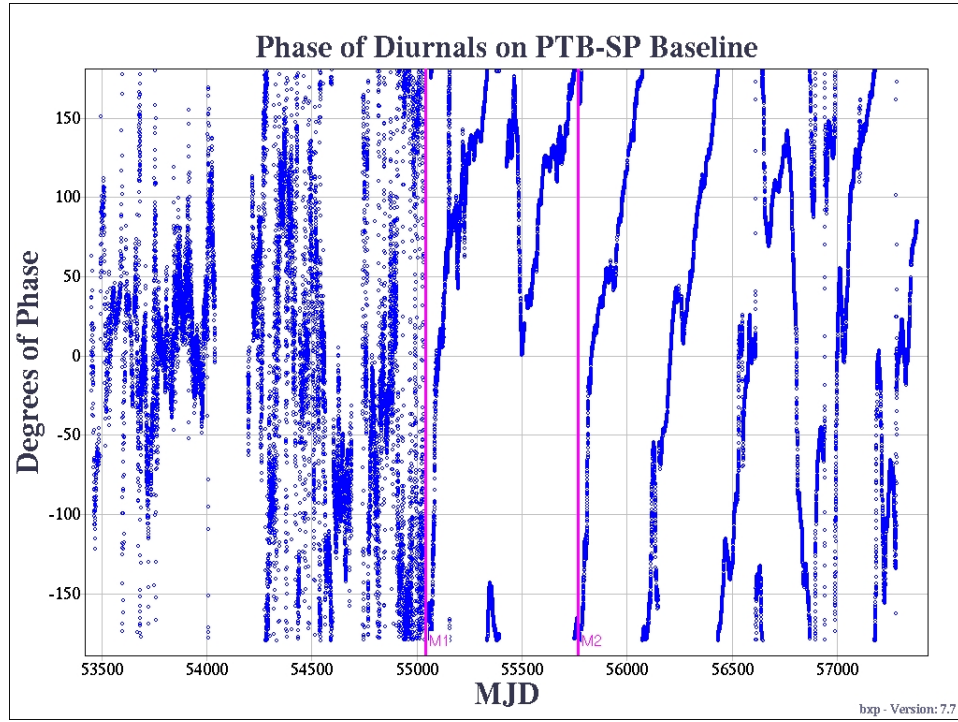


Figure 17. Phase of diurnals between the Swedish lab SP and the German lab PTB. The marker on MJD 50042 indicates a considerable change in the pattern when the bandwidth and chip rate were reduced. The marker on MJD 55769 shows a possible change in the delay pattern when the bandwidth was further reduced. Most of the Europe-only baselines show a similar pattern. No attempt was made to adjust for the 360-degree phase ambiguity.

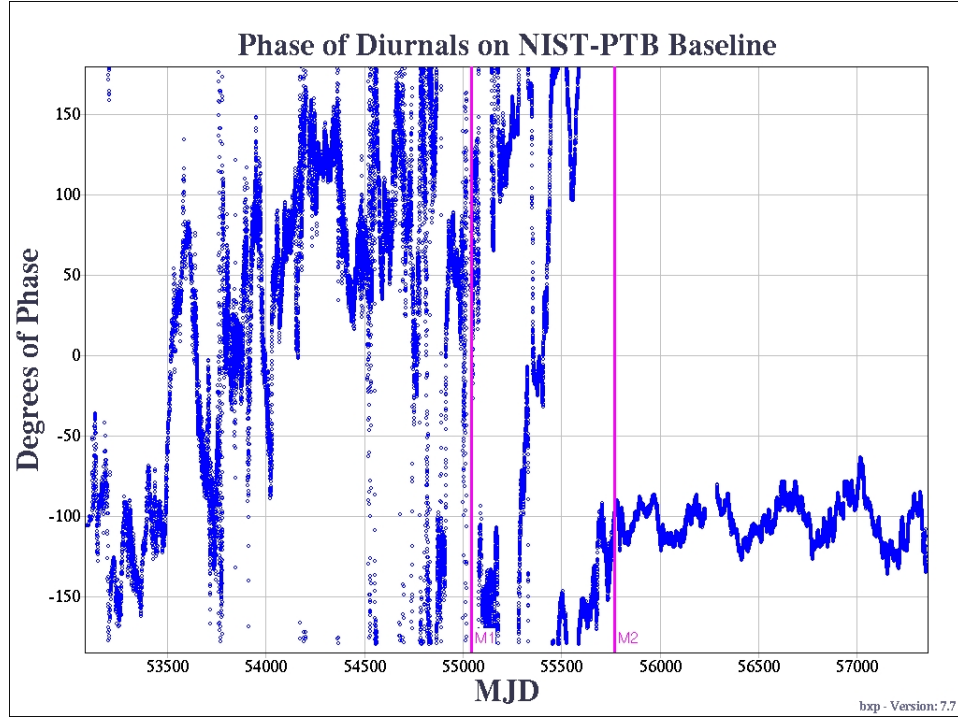


Figure 18. Phase of diurnals on the NIST-PTB baseline. While a change of pattern may have occurred after the bandwidth and chip rate reductions of MJD 55042, the marker on MJD 55769 shows that the further bandwidth reduction apparently had a larger effect. The USNO-PTB baseline shows a similar pattern.

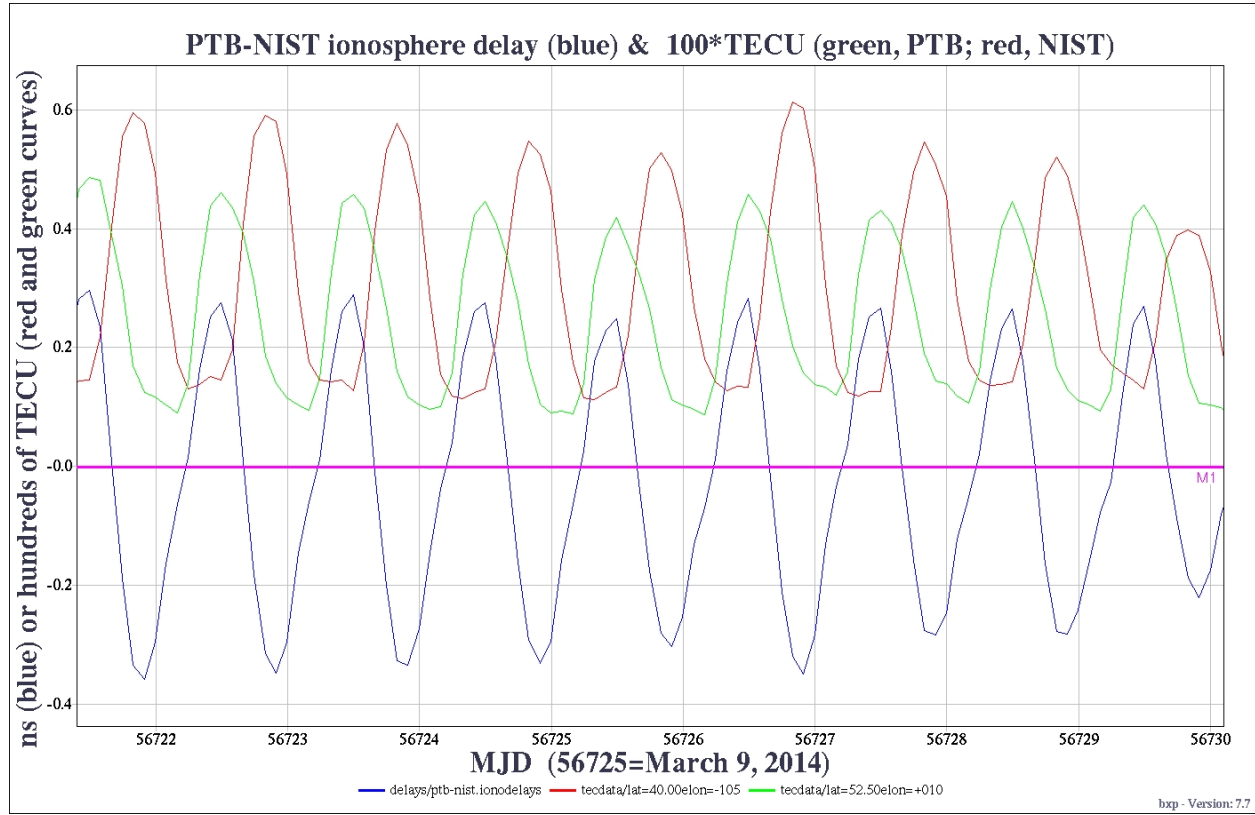


Figure 19. Diurnals expected due to uncorrected ionosphere errors on the trans-Atlantic PTB-NIST baseline, in ns units, at a period of high TEC. The green and red curves indicate the measured TEC values for PTB and NIST respectively, in units of hundreds of TECU. The expected delay also depends upon the satellite's slant angle, which in this case is 2.4 for PTB and 2.7 for NIST.